Supplementary Information for stereodynamical control of cold HD+ D_2 collisions

Bikramaditya Mandal,[1] James F. E. Croft,[2] Pablo G. Jambrina,[3]
Hua Guo,[4] F. Javier Aoiz,[5] and Naduvalath Balakrishnan[1]

[1] *Department of Chemistry and Biochemistry, University of Nevada, Las Vegas, Nevada 89154, USA*
[2] *Department of Chemistry, Durham University, South Road, Durham, DH1 3LE, United Kingdom*
[3] *Departamento de Química Física, University of Salamanca, Salamanca 37008, Spain*
[4] *Department of Chemistry and Chemical Biology, University of New Mexico, Albuquerque, New Mexico 87131, USA*
[5] *Departamento de Química Física, Universidad Complutense, Madrid 28040, Spain*

Scattering calculations of HD+D_2 collisions were carried out using two highly accurate full-dimensional potential energy surfaces (PESs) for the H_2-H_2 system, namely the Zuo, Croft, Yao, Balakrishnan, and Guo (ZCYBG) PES [1] and the Hinde PES [2]. While some comparisons of cross sections for rotationally inelastic collisions on the two PESs are presented in the main article, comparisons with experimental data are provided only for the ZCYBG PES. Here, for completeness and for future reference, we provide similar comparisons on the Hinde PES which depict nearly identical results. Additional results of velocity-dependent differential rate coefficients for H-SARP and V-SARP preparations of the HD molecules are presented for both PESs.

[1] J. Zuo, J. F. E. Croft, Q. Yao, N. Balakrishnan and H. Guo, *Journal of Chemical Theory and Computation*, 2021, **17**, 6747.
[2] R. J. Hinde, *The Journal of Chemical Physics*, 2008, **128**, 154308.
[3] U. Buck, F. Huisken, J. Schleusener and J. Schaefer, *The Journal of Chemical Physics*, 1981, **74**, 535.
[4] U. Buck, F. Huisken, G. Maneke and J. Schaefer, *The Journal of Chemical Physics*, 1983, **78**, 4430.
[5] W. E. Perreault, N. Mukherjee and R. N. Zare, *Science*, 2017, **358**, 356.
[6] W. E. Perreault, N. Mukherjee and R. N. Zare, *Nature Chemistry*, 2018, **10**, 561.

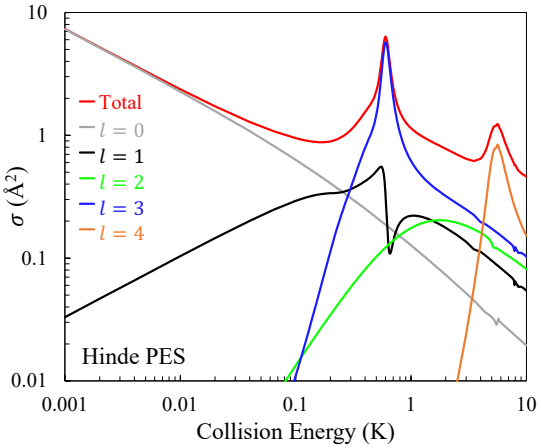

Fig. S1. Partial wave-resolved cross sections for the rotational transition $j_{\rm HD} = 2 \rightarrow j'_{\rm HD} = 0$ in HD in collisions with $D_2(j = 0)$ as a function of the collision energy evaluated on the Hinde PES. The red curve denotes the total quenching cross section while grey, black, green, blue and orange curves show contributions from $l = 0, 1, 2, 3$, and 4 respectively. It can be seen that the primary peak is due to $l = 3$ while the secondary peak arises from $l = 4$.

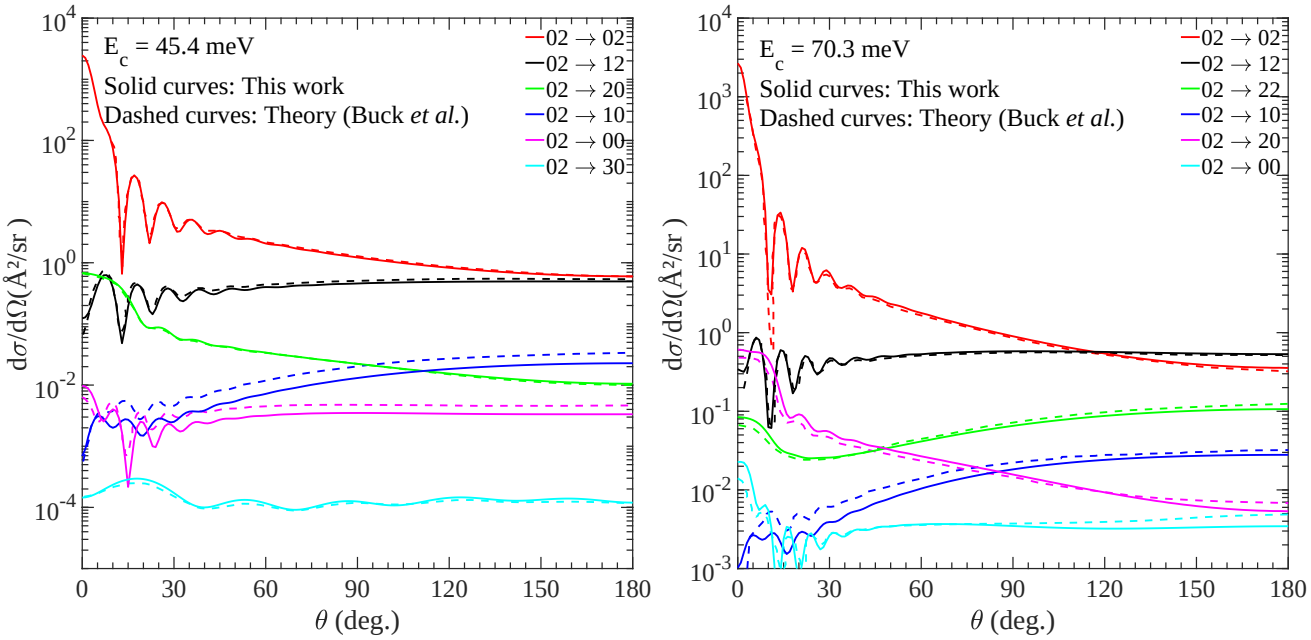

Fig. S2. Comparison of angular dependence of the differential cross sections from our calculations using the Hinde PES (solid lines) and those reported by Buck et al. [3, 4] (dashed lines) for state-to-state transitions (refer to the legends inside figure) at collision energies of 45.4 meV (left panel) and 70.3 meV (right panel). The transitions are denoted as $j_{\mathrm{HD}} j_{\mathrm{D_2}} \rightarrow j'_{\mathrm{HD}} j'_{\mathrm{D_2}}$.

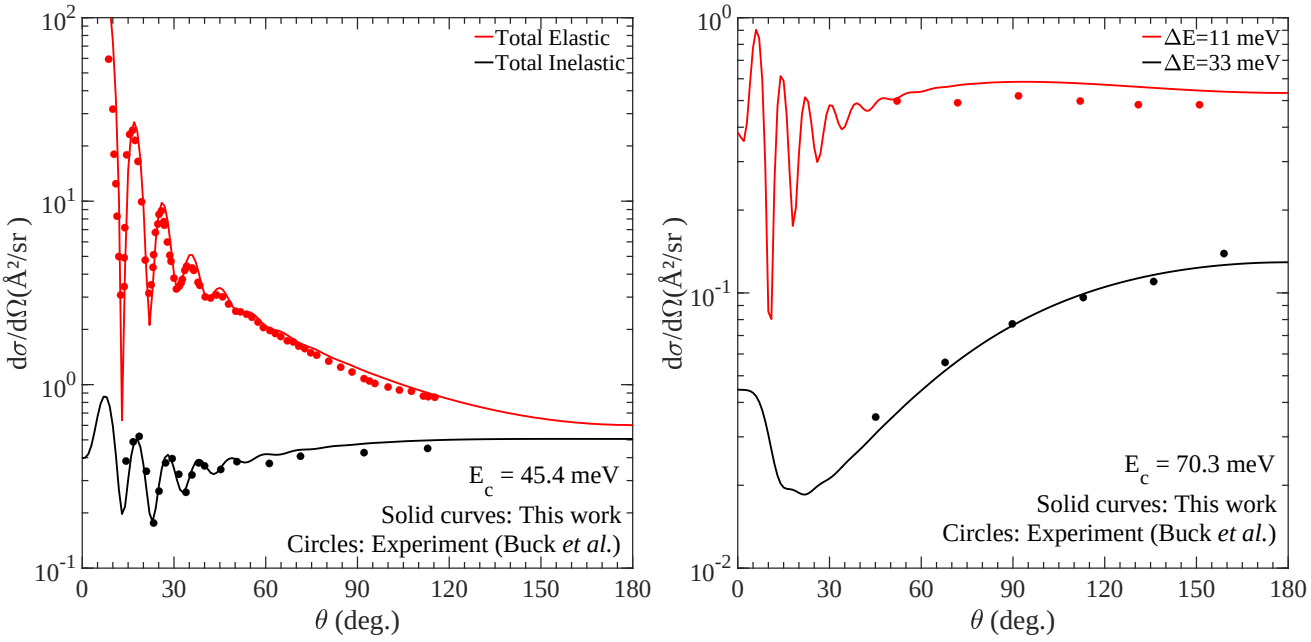

Fig. S3. Comparison of angular dependence of the total elastic and inelastic differential cross sections from our calculations on the Hinde PES (solid curves) and experimental data of Buck et al. (circles) at collision energies of 45.4 meV (left panel) and 70.3 meV (right panel). See the main article for details.

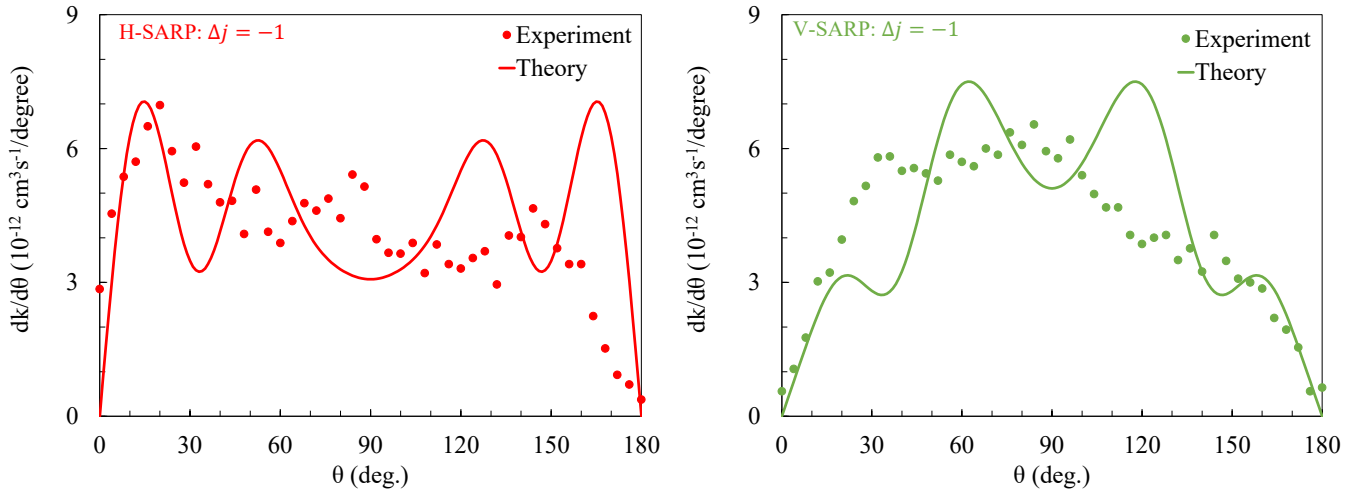

Fig. S4. A comparison between experiment and theory for the angular distribution of the velocity averaged differential rate coefficient for rotational quenching of HD for the $j_{\rm HD} = 2 \rightarrow j'_{\rm HD} = 1$ transition. The left and right panels correspond to H-SARP and V-SARP preparations, respectively. The experimental data of Perreault et al. [5] are shown by filled circles while the theoretical results are shown by solid and dashed curves as labeled in the legend.

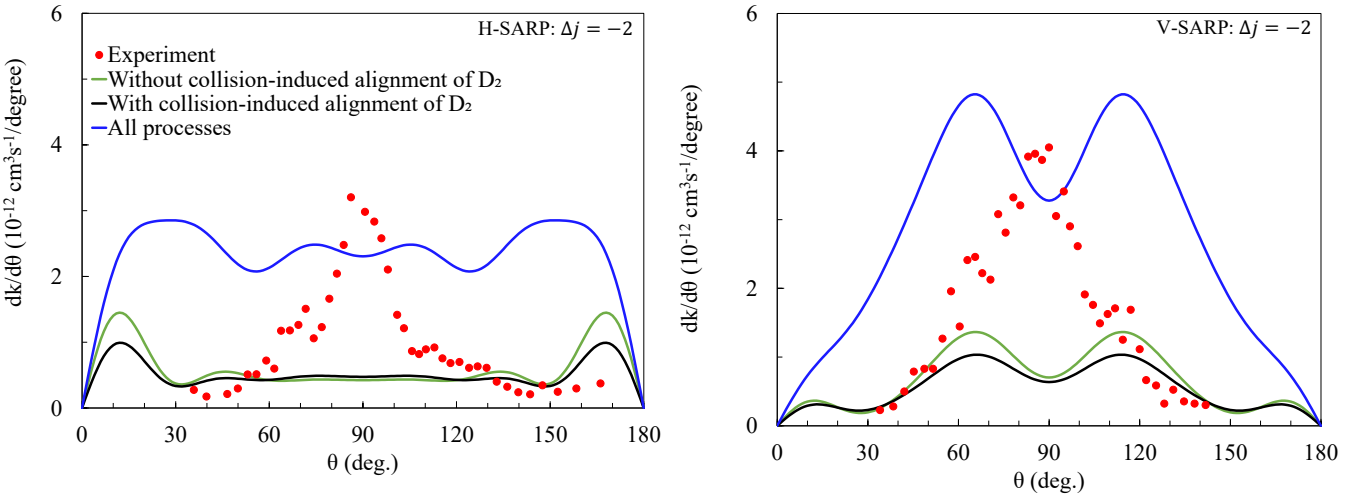

Fig. S5. Differential rate coefficients for $j_{\rm HD} = 2 \rightarrow j'_{\rm HD} = 0$ rotational transition in HD induced by collisions with D_2. Results for H-SARP (left panel) and V-SARP (right panel) preparations of the HD molecule from Perreault et al. [6] (red dots) are compared against theoretical results (solid curves) from this work. Black and green curves denote theoretical results with and without collision-induced alignment of $D_2(j = 1)$, respectively, while the blue curve includes the effect of collision-induced alignment of $D_2(j = 1)$ and D_2 excitation from $j = 0 \rightarrow j' = 2$.

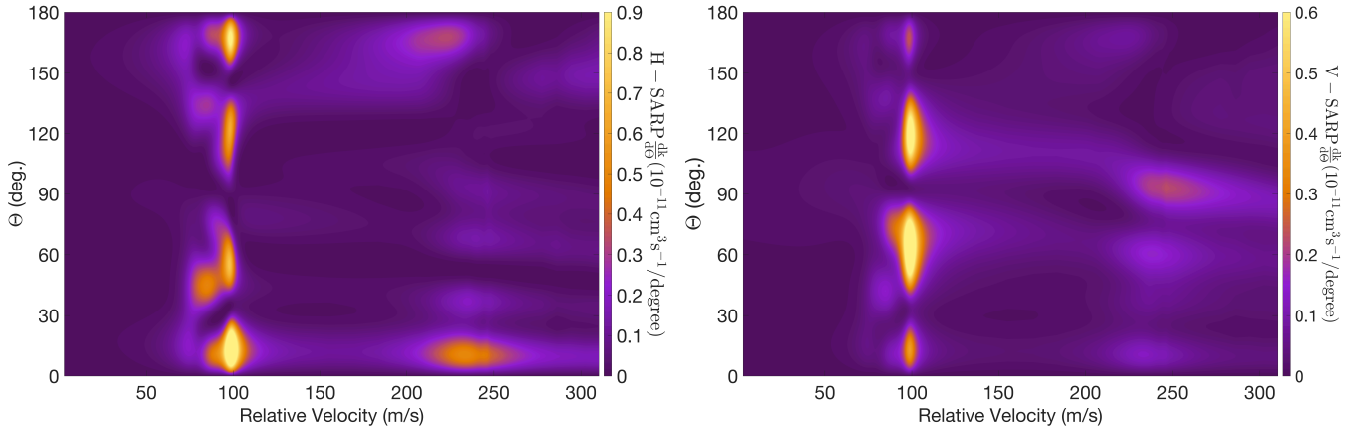

Fig. S6. Differential state-to-state rate coefficients for the transition HD($v = 1, j = 2$) → HD($v' = 1, j' = 0$) in collisions with *ortho*-D_2($j = 0$) for the V-SARP (upper panel) and H-SARP (lower panel) preparations of the HD molecule computed using the ZCYBG PES. [1]. Contributions from the rotational excitation of D_2($j = 0$) is not included in this result.

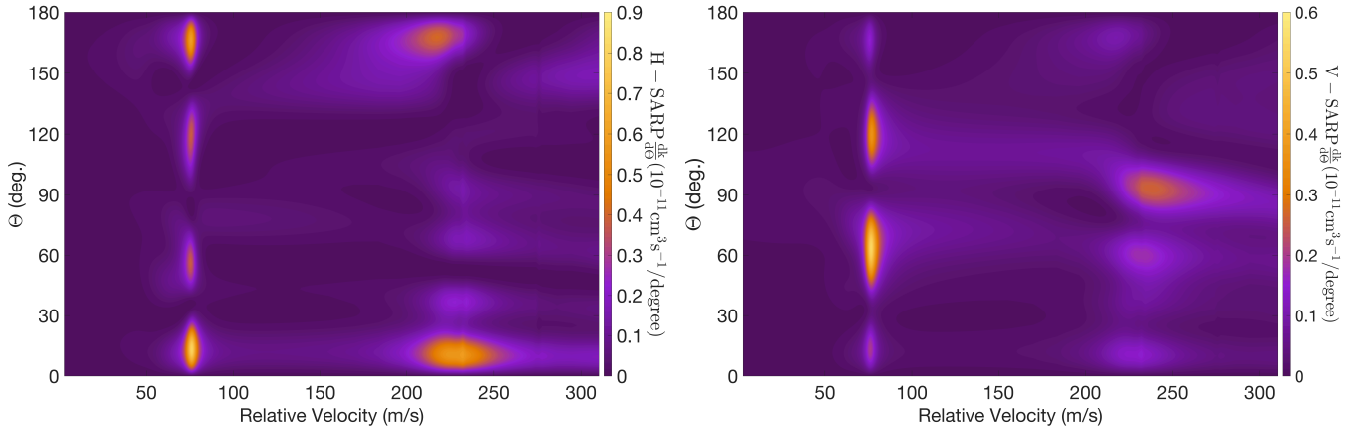

Fig. S7. The same as Figure S6, but using the Hinde PES.

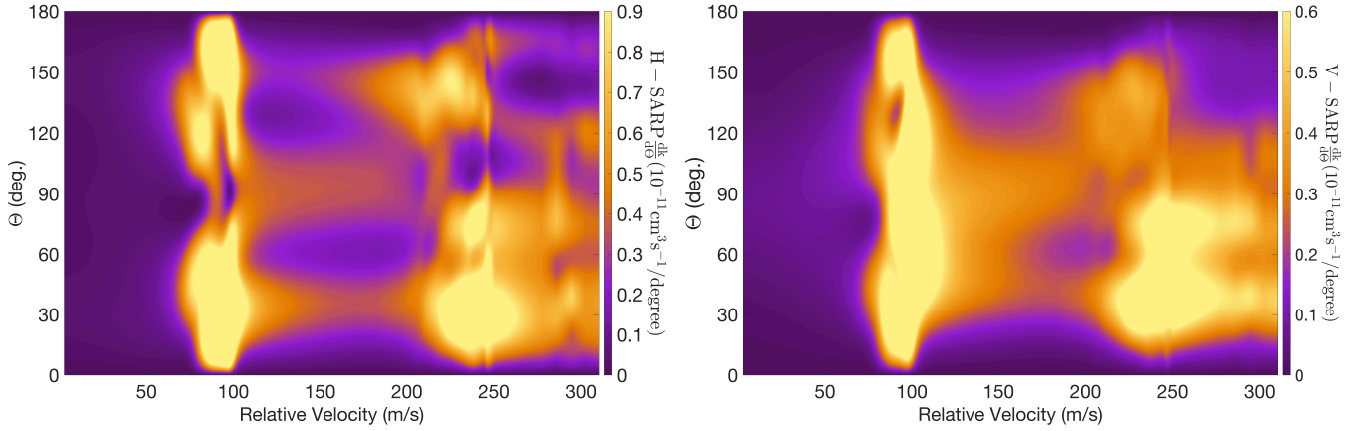

Fig. S8. Differential state-to-state rate coefficients for the transition HD($v = 1, j = 2$) → HD($v' = 1, j' = 0$) that include concurrent excitation of *ortho*-D_2 ($v = 0, j = 0$) → ($v' = 0, j' = 2$) for the V-SARP (upper panel) and H-SARP (lower panel) preparations of the HD molecule computed using the ZCYBG PES.

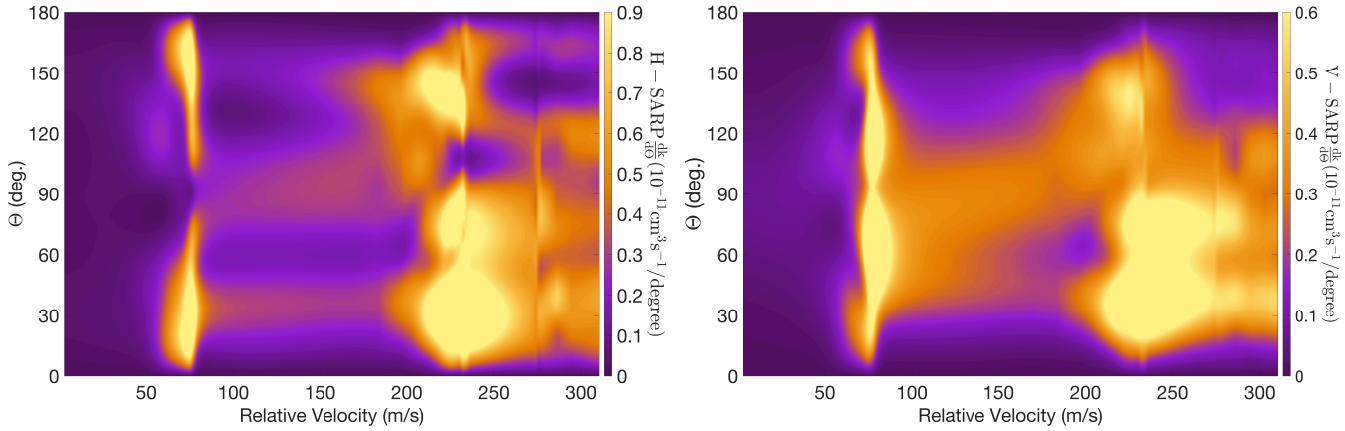

Fig. S9. Same as Figure S8, but using the Hinde PES.

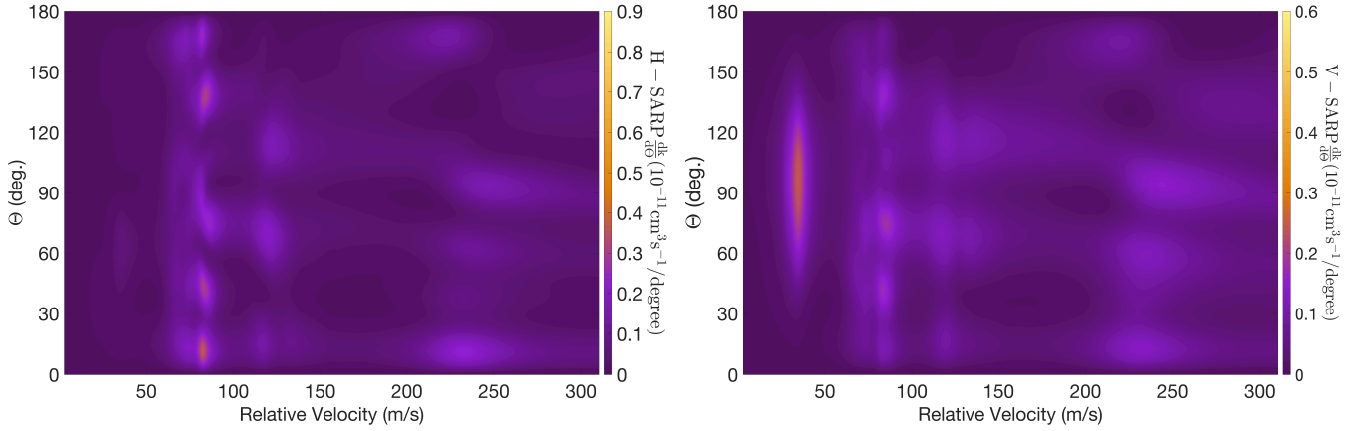

Fig. S10. Differential state-to-state rate coefficients for the transition HD($v = 1, j = 2$) $\rightarrow$ HD($v' = 1, j' = 0$) in collisions with *para*-D_2($j = 1$) for the V-SARP (upper panel) and H-SARP (lower panel) preparations of the HD molecule using the ZCYBG PES.

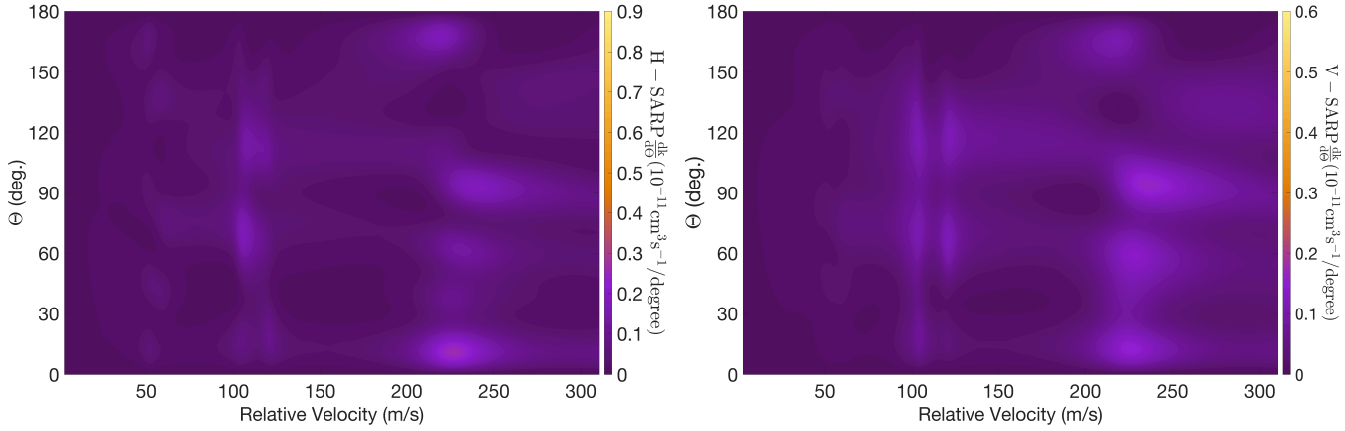

Fig. S11. Same as Figure S10, but using the Hinde PES.